

SATURN HISTORY DOCUMENT
University of Alabama Research Institute
History of Science & Technology Group

Date ----- Doc. No. -----

NOISE REDUCTION STUDY IN A SCALED MODEL
ACOUSTIC TEST FACILITY

BY

R. H. TOMREN

BROWN ENGINEERING, A TELEDYNE COMPANY
HUNTSVILLE, ALABAMA

PREPARED FOR

75TH MEETING OF THE ACOUSTICAL
SOCIETY OF AMERICA
OTTAWA, ONTARIO, CANADA

MAY 21-24, 1968

LIST OF SYMBOLS

a, t	Subscripts indicating absorption and transmission
α_i	Acoustical energy absorption coefficient
$\bar{\alpha}_t(f)$	Total equivalent statistical absorption coefficient
	$\frac{1}{S_a} \left[\sum_i \alpha_i S_i + \frac{4}{\mu} (f) V \right]$
c	Speed of sound
c_1	Anechoic room correction
c_2	Ambient air correction
f	Frequency
K(m)	Absorption characteristic of anechoic room as a function of meteorological conditions.
log	Log 10
NR	Noise reduction
ρc	Characteristic acoustic impedance of air
$\rho_o c_o$	Characteristic acoustic impedance of air at sea level
SPL _R	Sound pressure level, reverberant
SPL _A	Sound pressure level, anechoic
TL	Transmission loss

SUMMARY

The acoustic properties of five insulation materials were investigated in a 1/10-scale model acoustic facility. The materials were designed for applications in space vehicles. The model facility, consisting of a reverberation chamber coupled to an anechoic chamber, was evaluated for its use in noise reduction testing. It was found that a reasonably diffuse sound field existed above 900 Hertz. Modal density graphs of the reverberation chamber and spatial acoustic gradients measured within the chamber and across the test panel opening are compared to an idealized facility.

INTRODUCTION

The noise reduction (NR) is defined as the difference between the sound pressure levels (in decibels) on the two sides of the panel. It is essential to realize that noise reduction and transmission loss (TL) are different quantities. Transmission loss (TL) in decibels is defined as $10 \log_{10}$ of the ratio of the acoustic intensity (acoustic power per unit area) incident upon the test sample, to the acoustic intensity transmitted through it. There are a number of methods for measuring the transmission loss of a test sample in a laboratory, reference 1. Currently the two methods for determining the transmission loss of a panel used for this paper are (1) experimental measurement and (2) theoretical prediction. To obtain the transmission loss of the panel experimentally, one may use data obtained by placing a panel between a reverberant chamber and an anechoic or semi-reverberant chamber.

$$\text{Noise Reduction (NR)} = \text{SPL}_R - \text{SPL}_A$$

Transmission loss (TL) can be obtained by using,

$$\text{TL} = \text{NR} - K(m)$$

where $K(m)$ is the absorption characteristic of the anechoic room as a function of meteorological conditions. This information should be available in the form of curves made when the facility was calibrated.

In the absence of calibration data, one uses:

$$K(m) = C_1 + C_2, \text{ reference 2.}$$

where C_1 = correction for the effects of the anechoic or semi-reverberant room

$$\left(-10 \log \left[\frac{S_t}{S_a} \left(\frac{1 - \bar{\alpha}}{\bar{\alpha}} \frac{t(f)}{t(f)} \right) \right] \right) \text{ Reference 2.}$$

C_2 = correction for ambient conditions within the anechoic or semi-reverberant room.

$$\left(20 \log \left(\frac{\rho_o c_o}{\rho c} \right) \right) \text{ Reference 2.}$$

The theoretical approach, as used, is neither as straightforward nor as accurate as the experimental. In obtaining a theoretical TL curve, the first step is to divide the transmission loss curve into five regions. This allows for the different effects of various physical properties associated with each region to be considered.

- Region 1. Panel motion dictated by panel stiffness and support.
- Region 2. Panel motion dictated by panel resonances.
- Region 3. Panel motion dictated predominantly by the weight of the panel surface.
- Region 4. Panel motion dictated to some extent by coincidence effect.
- Region 5. Panel motion dictated by multi-modal effects.

The regions in the preceding list refer to consecutive portions of the curve with Region 1 at the low frequency end. These regions may overlap. Region 3 is commonly referred to as the "mass law" region. Most of the experimental data, obtained in these tests, apply to the mass law region.

Several aerospace insulation materials were investigated for acoustic properties. The materials were all possible candidates for blanket covering protection of the Electron Beam Welder (EBW) package, an experiment for the S-IVB Orbital Workshop mission. One insulation material was to be selected for future application involving qualification testing and flight hardware configuration, reference 3.

I. PROGRAM DESCRIPTION

The purpose of this program was to investigate the noise reduction properties of several possible insulation materials for the EBW package and select one material for application as an acoustic blanket protector. The EBW package will be located in the multiple docking adapter (MDA). The package is one of several experiments for the S-IVB Orbital Workshop missions. The workshop is part of the Apollo Application Program (AAP), reference 3.

Five test specimens were designed and fabricated for development testing in the 1/10-scale dynamic acoustic model facility. (See figure 1.) The model facility consists of a reverberation chamber coupled to an anechoic chamber. The scale model facility is quite limited in its use for noise reduction (NR) testing. The reasons for these limitations are as follows:

(1) There is a reasonably diffuse sound field above 900 Hz., reference 4. It might be noted that the sound field in a reverberant chamber should be considered diffuse before the normal statistical equations predicting sound pressure levels are applied. Various "rules of thumb" may be used to determine the minimum frequency at which the sound field becomes diffuse, but no formal method has been devised for measuring diffusivity. It may be inferred from a measure of modal density, spatial gradients, or spatial correlation of the sound field; however, none of these parameters directly indicates that equal energy in each frequency band is arriving at a particular point from all directions simultaneously (one definition of diffusivity), references 1 and 4.

(2) In reference 4, modal density figures show a continuous succession of deep dips, 25 to 50 cycles wide, across the entire frequency band. These broad bands of low level are the result of the nearly cubical shape of the chamber. These dips have not been completely compensated for by the splayed walls so that equal energy per cycle criteria for diffusivity are not met in the room.

(3) In reference 4, spatial acoustic gradients were measured within the reverberation chamber and across the test panel opening. The normal variation appears in the low frequency region, but also a 3- to 5-decibel variation appears in the high frequency regions where 1- to 2-decibel would be more normal for a diffuse field.

(4) In reference 4, typical correlograms taken in the reverberation chamber are given. The function $(\sin kx)/kx$ is plotted on each graph using the first zero crossing as a matching point. Correlation was performed on the full band of energy available in the room. The criterion that sound is arriving from all directions at once would imply that the correlogram would follow the $\sin kx/kx$ function. One figure shows good coincidence in the X axis correlation, but other figures, in the other directions, show poor agreement.

(5) In reference 4, panel correlation comparisons were made. Correlograms, made across the vertical and horizontal centers of the test panel, give poor results.

II. SPECIMEN TESTING

The test specimens used were square panels. Each specimen was placed in the reverberation chamber of the model facility as shown in figures 2 and 3. Each specimen was exposed to a sinusoidal sweep and random acoustic excitation of sufficient duration that a steady state condition existed. Data were gathered from each steady state condition in both chambers of the facility and for each specimen. A description of the five specimens tested is shown in table 1.

Table 1

<u>Number</u>	<u>Description</u>
1.	Beta Cloth and Beta Mat (figure 4) 20" x 20" x 1/2" - two layers - SK30-3537
2.	Beta Cloth and Astroquartz (figure 5) 20" x 20" x 1.2" - three layers - SK30-3535
3.	Multilayer Aluminum Foil and Dexiglass (figure 6) 19" x 19" x 1" - 100 layers - compressed - #0663
4.	Multilayer Aluminized Mylar and Urethane Foam (figure 7) 19" x 19" x 1" - 24 layers - plain - GAC-4
5.	Multilayer Aluminized Mylar and Urethane Foam (figure 8) 19" x 19" x 1" - 24 layers - with holes - GAC-4

One microphone was centrally located in each chamber. The random acoustic data for each test specimen were recorded for each chamber. The noise spectrum curves for each chamber are shown in figures 9 through 18. The noise reduction (NR) curve for test specimen 1 is shown in figure 19. The NR curve for specimen 1 is based on the difference between the two spectrums, figures 9 through 10. The material, beta cloth and beta mat, is fire resistant and easy to fabricate for blanket applications. The NR curve for test specimen 2 is shown on figure 20. The NR curve for specimen 2 is based on the difference between the two spectrums of figures 11 and 12. The material, beta cloth and astroquartz, is fire resistant and fairly easy to fabricate for blanket applications. Specimen 2 does not have the NR qualities for the higher frequencies that specimen 1 has. The NR curve for test specimen 3 is shown in figure 21. The NR curve for specimen 3 is based on the difference between the two spectrums of figures 13 and 14. The material, multilayer aluminum foil and dexiglass, is fire resistant but very difficult to fabricate for blanket applications. The material is extremely fragile and hard to work with. The NR curve for test specimen 4 is shown in figure 22. The NR curve for specimen 4 is based on the difference between the

two spectrums of figures 15 and 16. The material, multilayer aluminized mylar and urethane foam (without holes), is not fire resistant and does require special fabrication techniques. The material is quite rigid and would require a forming mandrel for the EBW package. The NR curve for test specimen 5 is shown in figure 23. The NR curve for specimen 5 is based on the difference between the two spectrums of figures 17 and 18. The material, multilayer aluminized mylar and urethane foam (with holes), is not fire resistant and does require special fabrication techniques. The material is quite rigid and would require a forming mandrel for the EBW package.

Table 2 is a summary of the five test specimens for random acoustic excitation. Specimens 1 and 2 are considered adequate materials for blanket covering. Specimen 1 is preferred because it is thinner than specimen 2. Use of specimen 1 would make fabrication and installation easier.

Table 2

Summary

<u>Test Specimen Number</u>	<u>Overall Noise Reduction (dB)</u>	<u>Weight lb/ft²</u>	<u>Ratio dB/lb/ft²</u>
1	38.5	.313	123
2	34.5	.164	210
3	40.0	.945	42.3
4	35.0	.278	126.
5	36.0	.275	131.

CONCLUSIONS

Sine sweep and random techniques were both used as input signals to the reverberation chamber. From reference 4, detailed analysis indicated the model reverberation chamber cutoff frequency was 300 Hz. and the first resonance was in excess of this. At the upper end of the frequency range, the dropoff was quite severe. Therefore, the most suitable and useful noise reduction data are in the range of 1000 Hz. and 5000 Hz. In terms of the full scale MSFC facility, this would be equivalent to the 100 Hz. to 500 Hz. range.

In evaluating the five test specimens for sound proofing ability and ease of manufacture, test specimens 1 and 2 are considered adequate for the EBW package. Specimen 1 is preferred because it is thinner than specimen 2. Use of specimen 1 would make fabrication and installation easier.

Because of the large size of the specimen and the small size of the model chamber, the qualitative NR values are of dubious value; however, for quantitative comparisons, the NR values are reasonable. The NR graphs follow the mass law theory quite well.

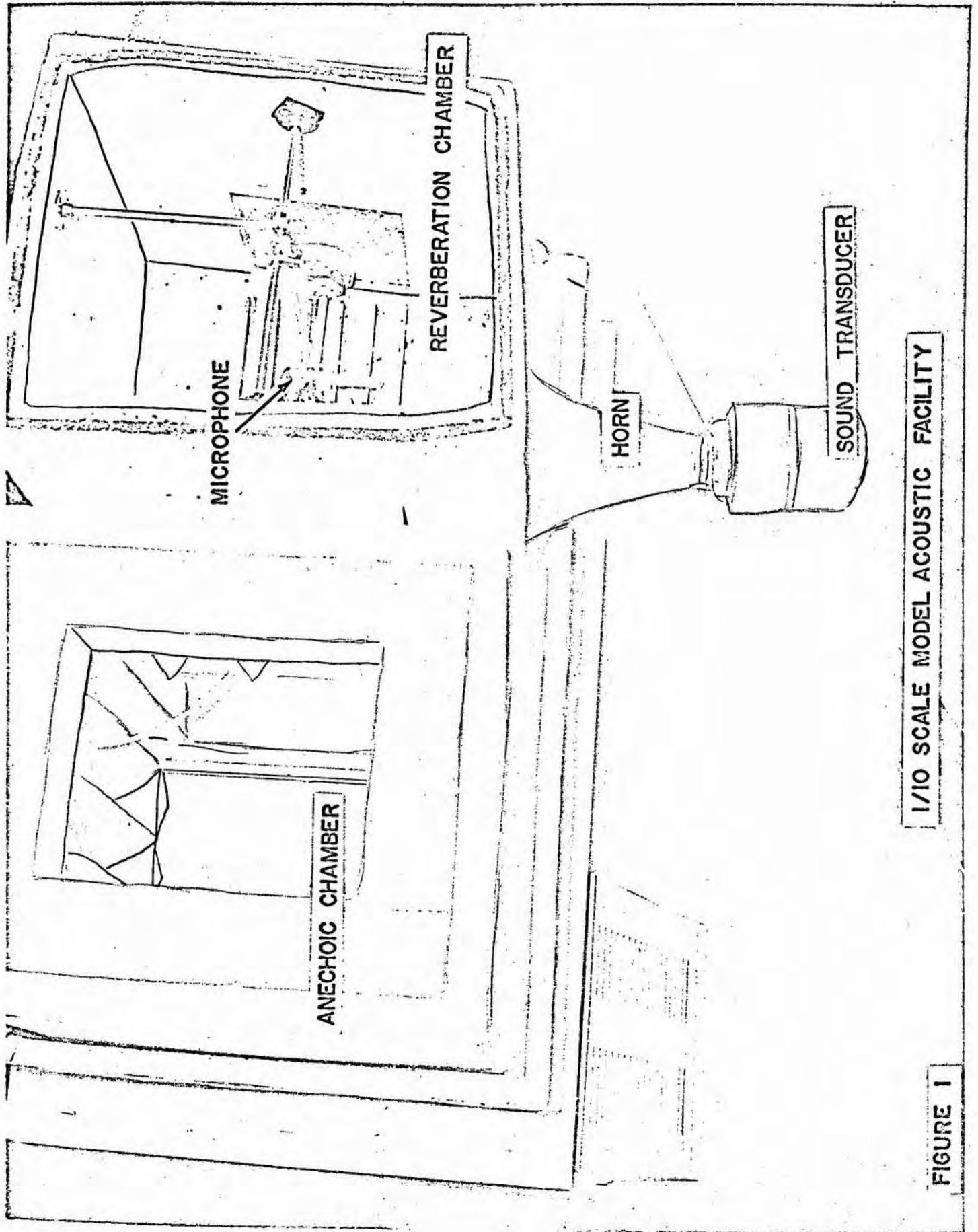
For future NR testing (where missile applications are involved), it is recommended that the full scale chambers be used. The very limited useful frequency range of the scale model would not be applicable to the full scale chambers. Also, the full scale chambers will have better sound field diffusivity characteristics.

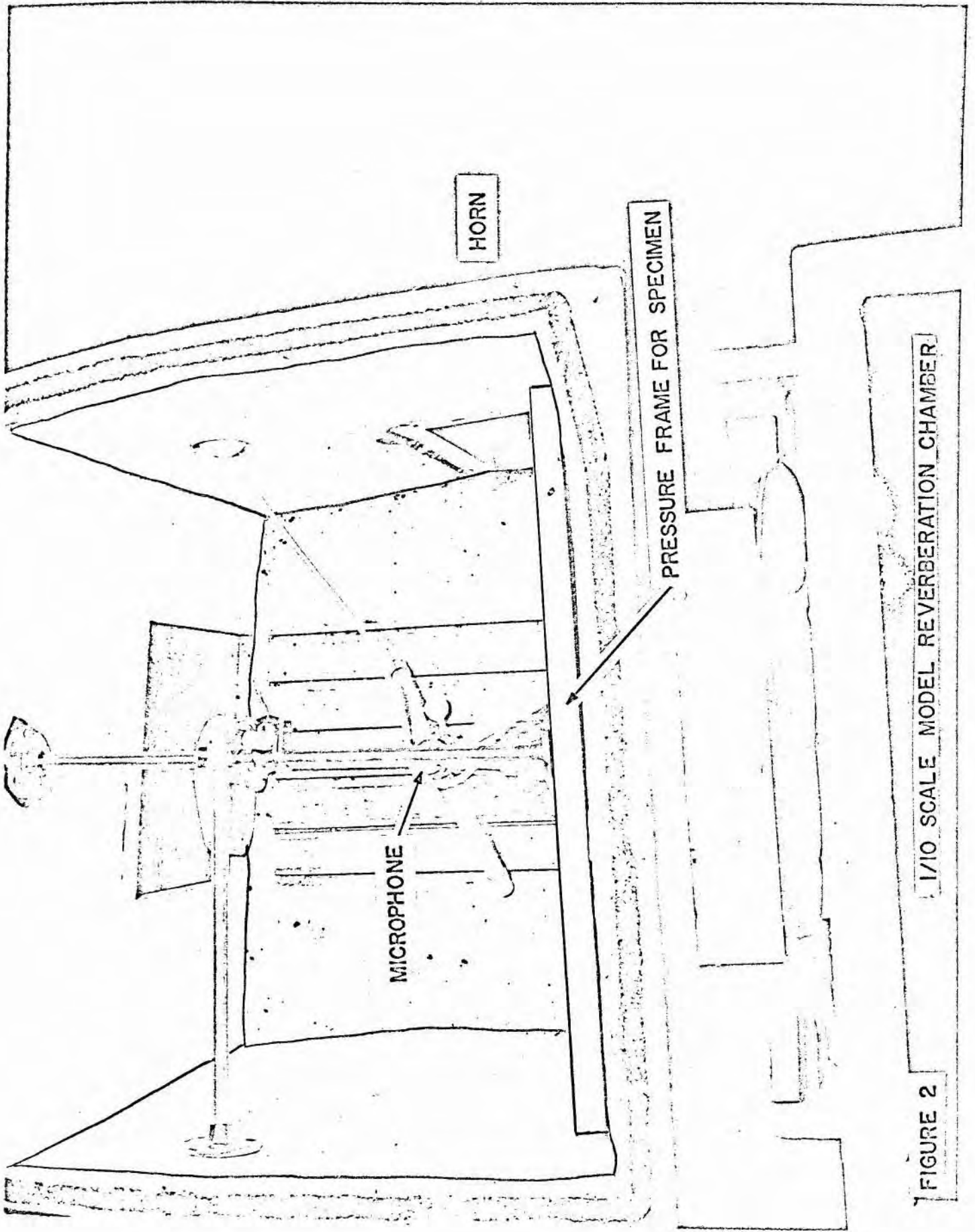
ACKNOWLEDGEMENT

This work was performed for the National Aeronautics and Space Administration at Marshall Space Flight Center under contract NAS8-20073.

REFERENCES

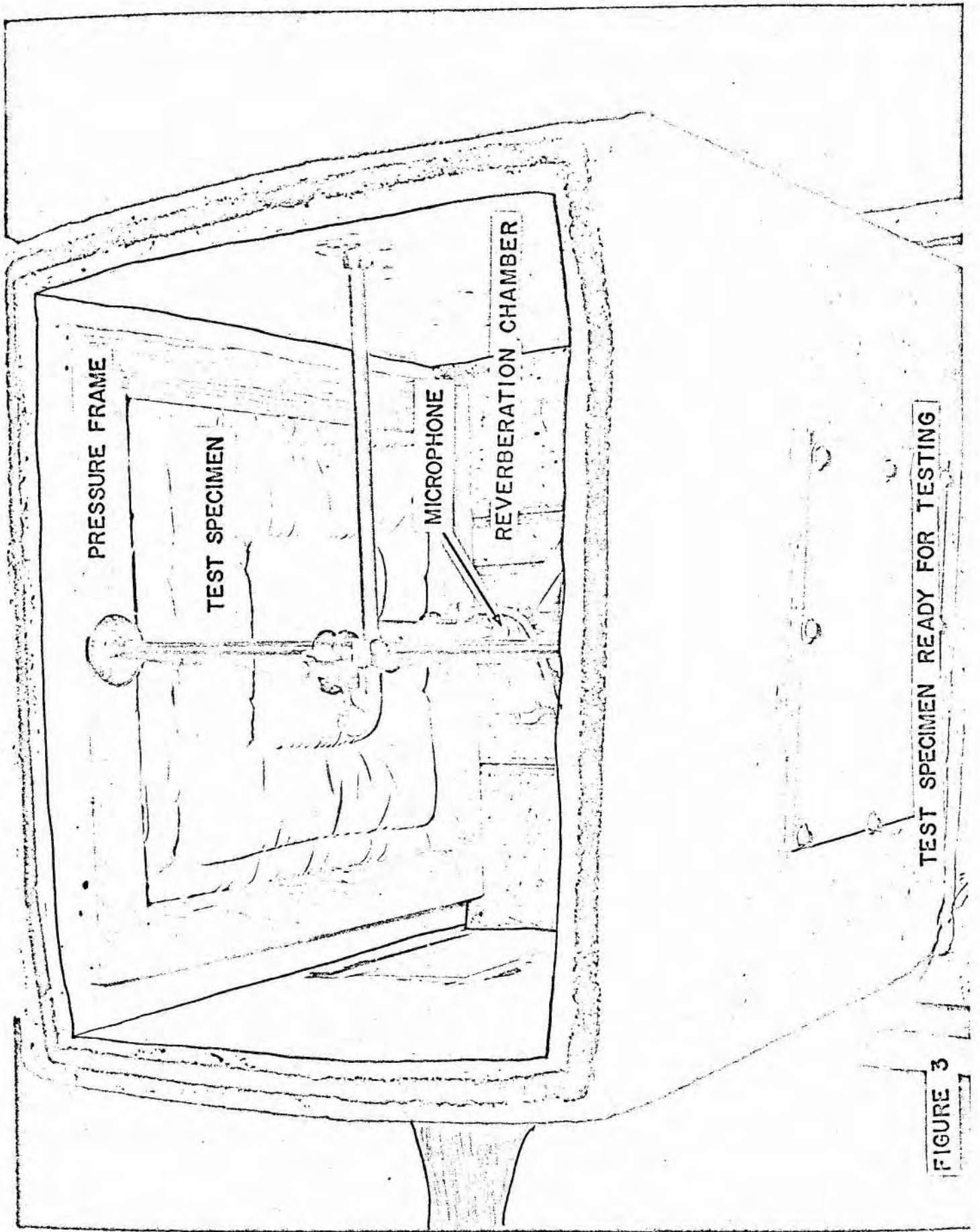
1. "Noise Reduction," Leo L. Beranek, McGraw-Hill: New York, 1960.
2. "Absorption of Sound in Air in the Audio-Frequency Range," J.A.S.A., Vol. 35, No. 1, January 1963.
3. "Noise Reduction Properties for Several Aerospace Insulation Materials," R.H. Tomren, Per Brandtzaeg, Brown Report 67-60.
4. "Acoustic Model Study of Reverberation Room Planned for Experimental Structures Laboratory," F. M. Murray, Wyle Report 65-14.





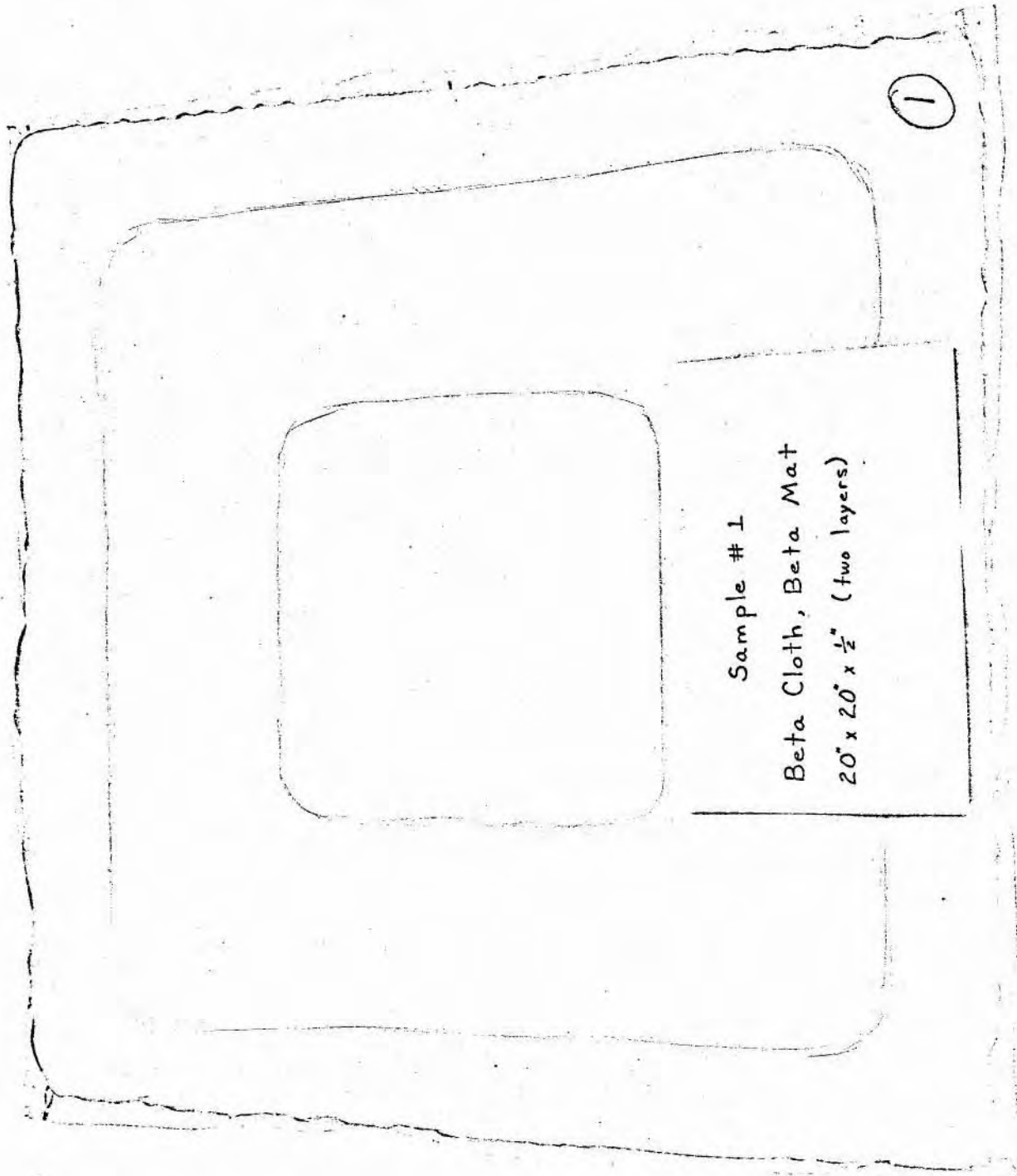
1/10 SCALE MODEL REVERBERATION CHAMBER

FIGURE 2



TEST SPECIMEN READY FOR TESTING

FIGURE 3



TEST SPECIMEN NO. 1 BETA CLOTH PLUS BETA MAT

FIGURE 4

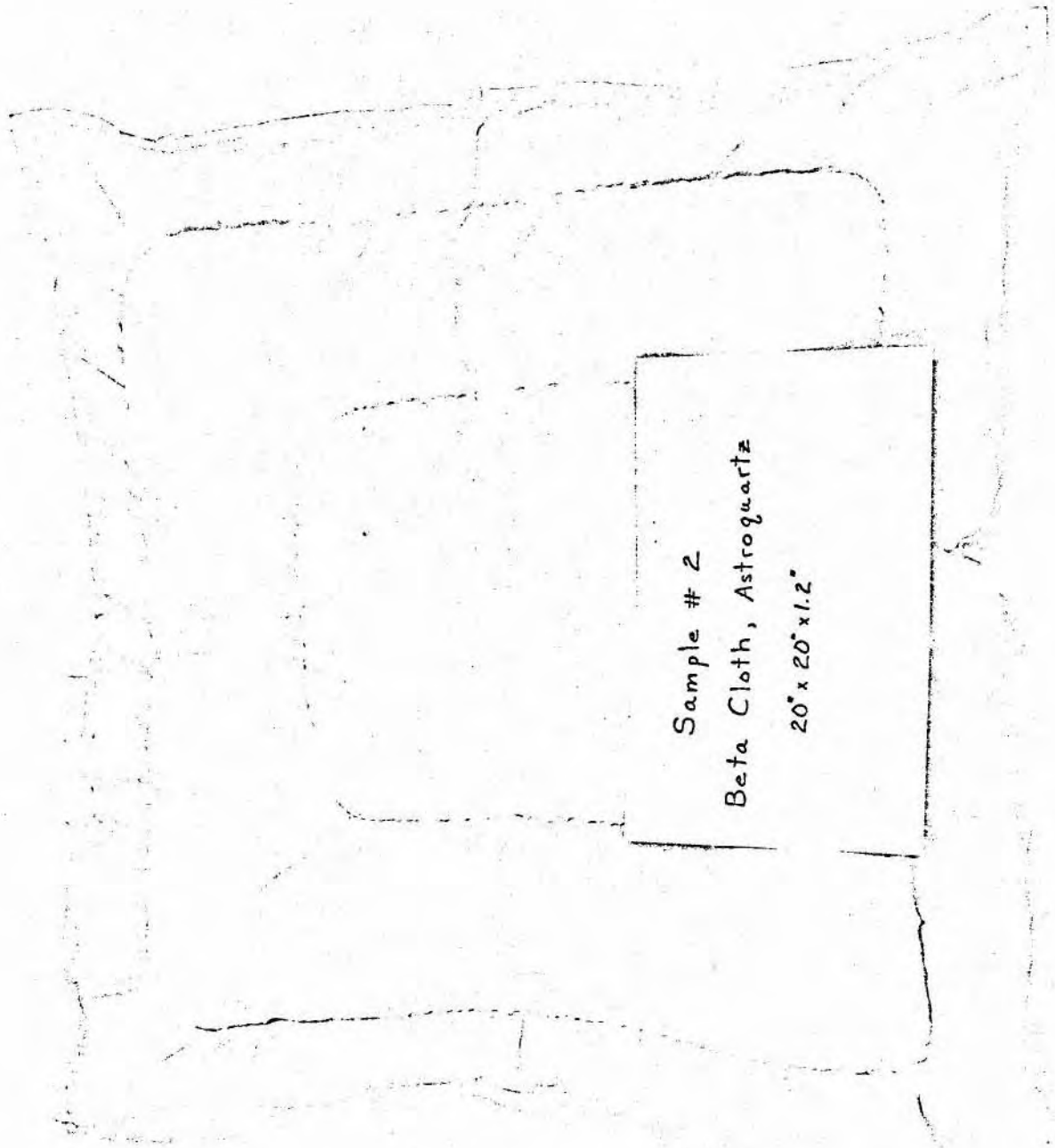


FIGURE 5

TEST SPECIMEN NO. 2 BETA CLOTH PLUS ASTROQUARTZ

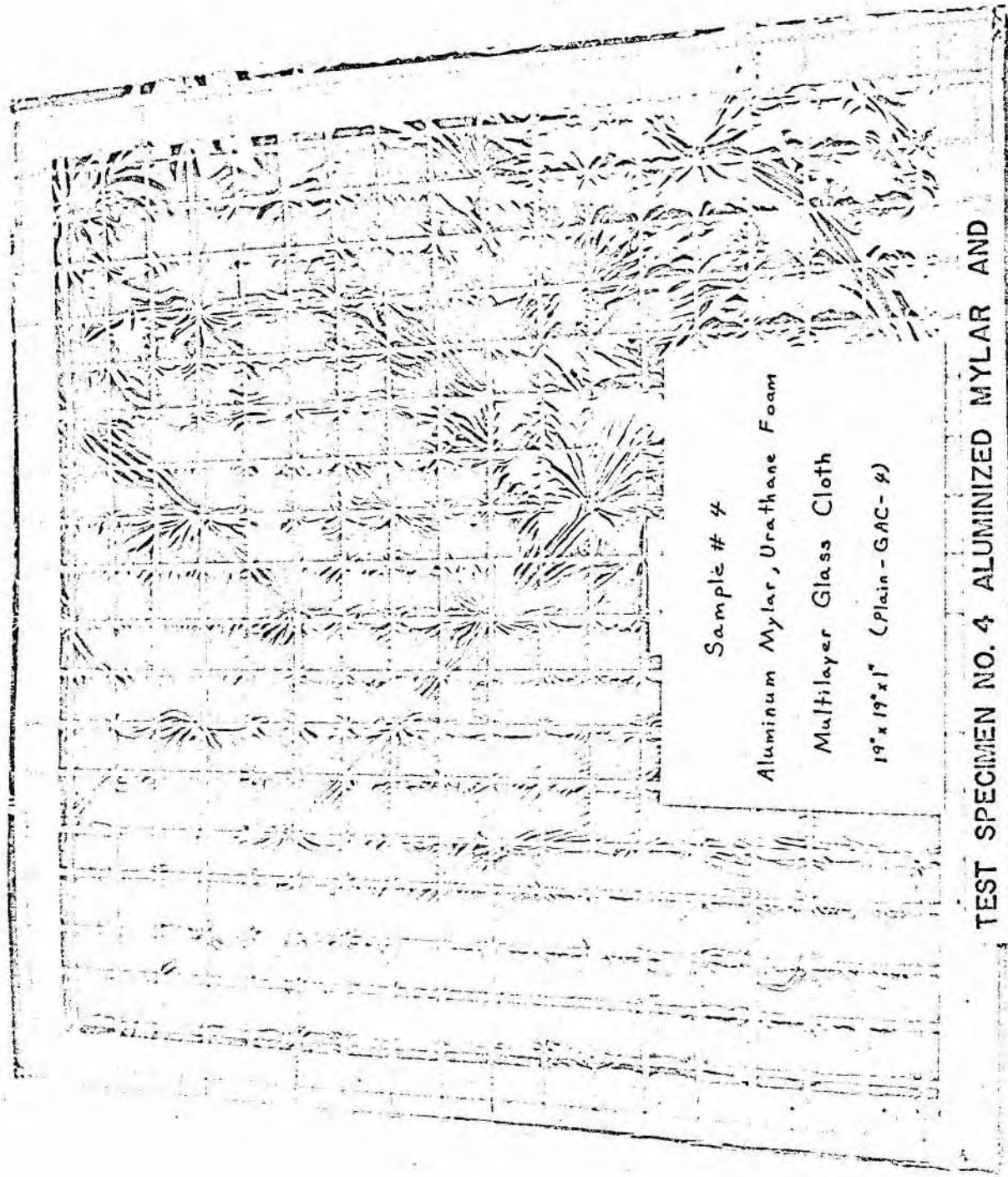


Sample # 3

Aluminum Foil, Dexiglass, Multilayer

19" x 19" x 1"

FIGURE 6 TEST SPECIMEN NO. 3 MULTILAYER ALUMINUM FOIL AND DEXIGLASS



URATHANE FOAM-PLAIN

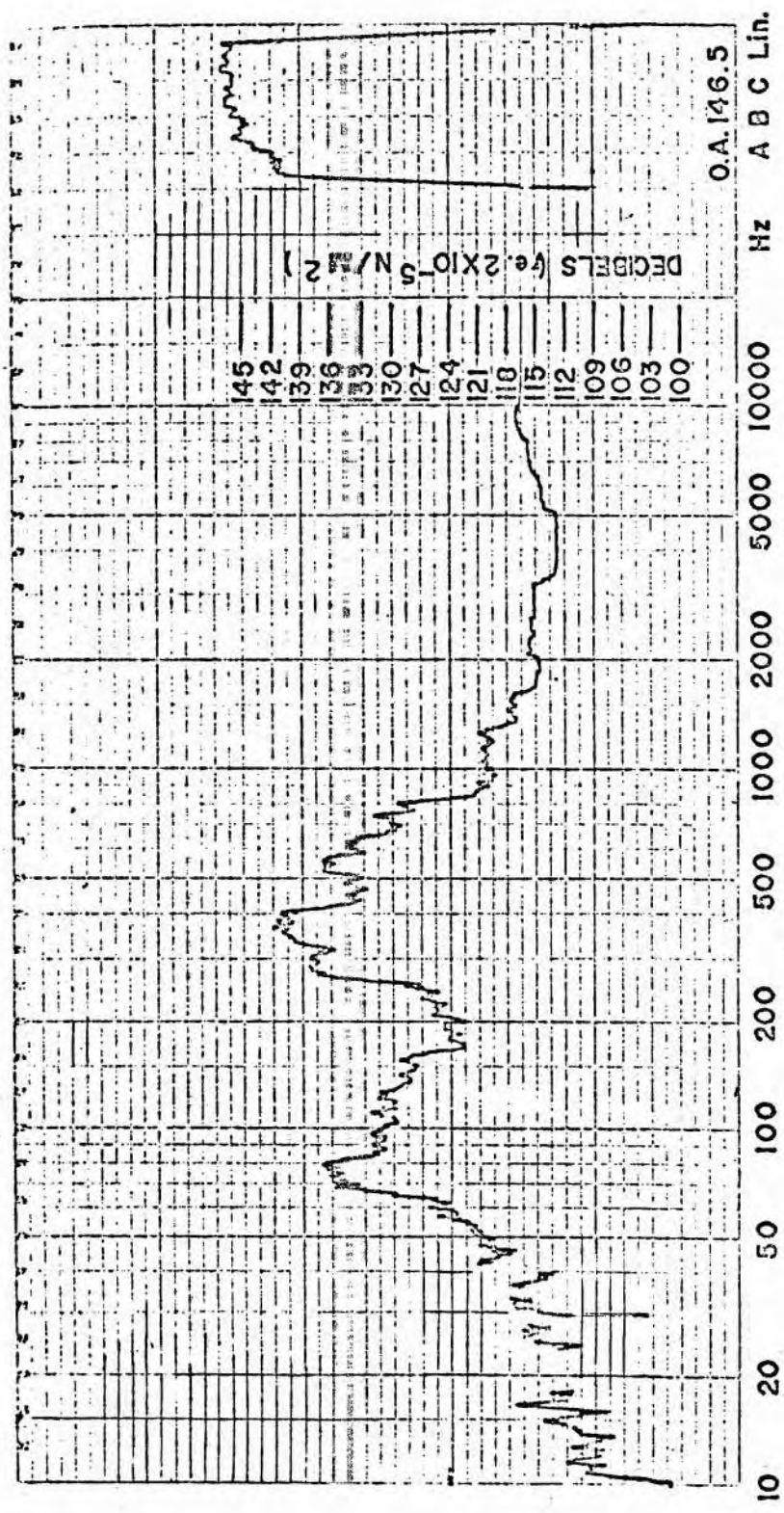
FIGURE 7



TEST SPECIMEN NO. 5 ALUMINIZED MYLAR AND URATHANE

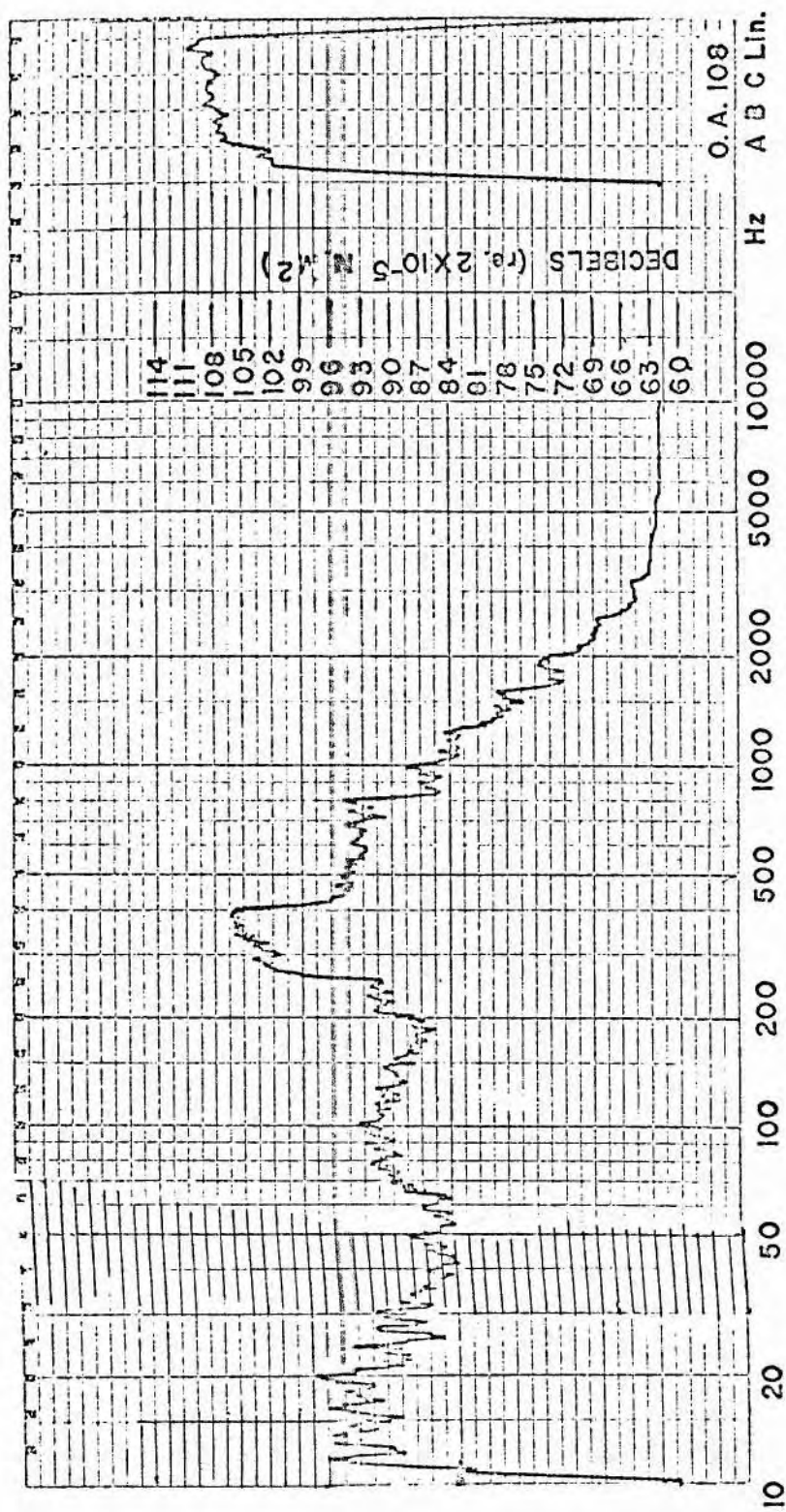
FOAM WITH HOLES

FIGURE 8



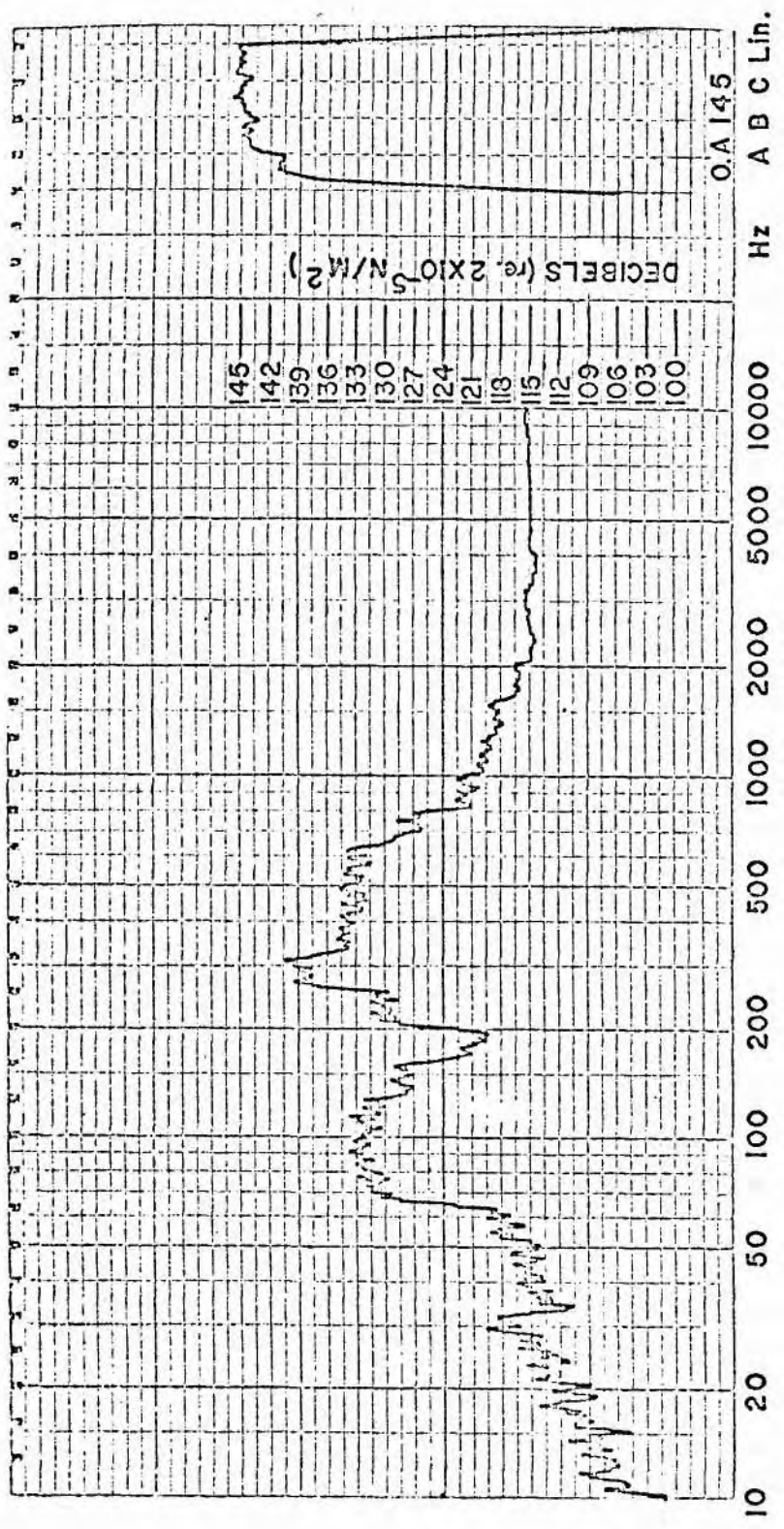
RANDOM NOISE SPECTRUM FOR TEST SPECIMEN NO. 1
IN REVERBERATION CHAMBER

FIGURE 9



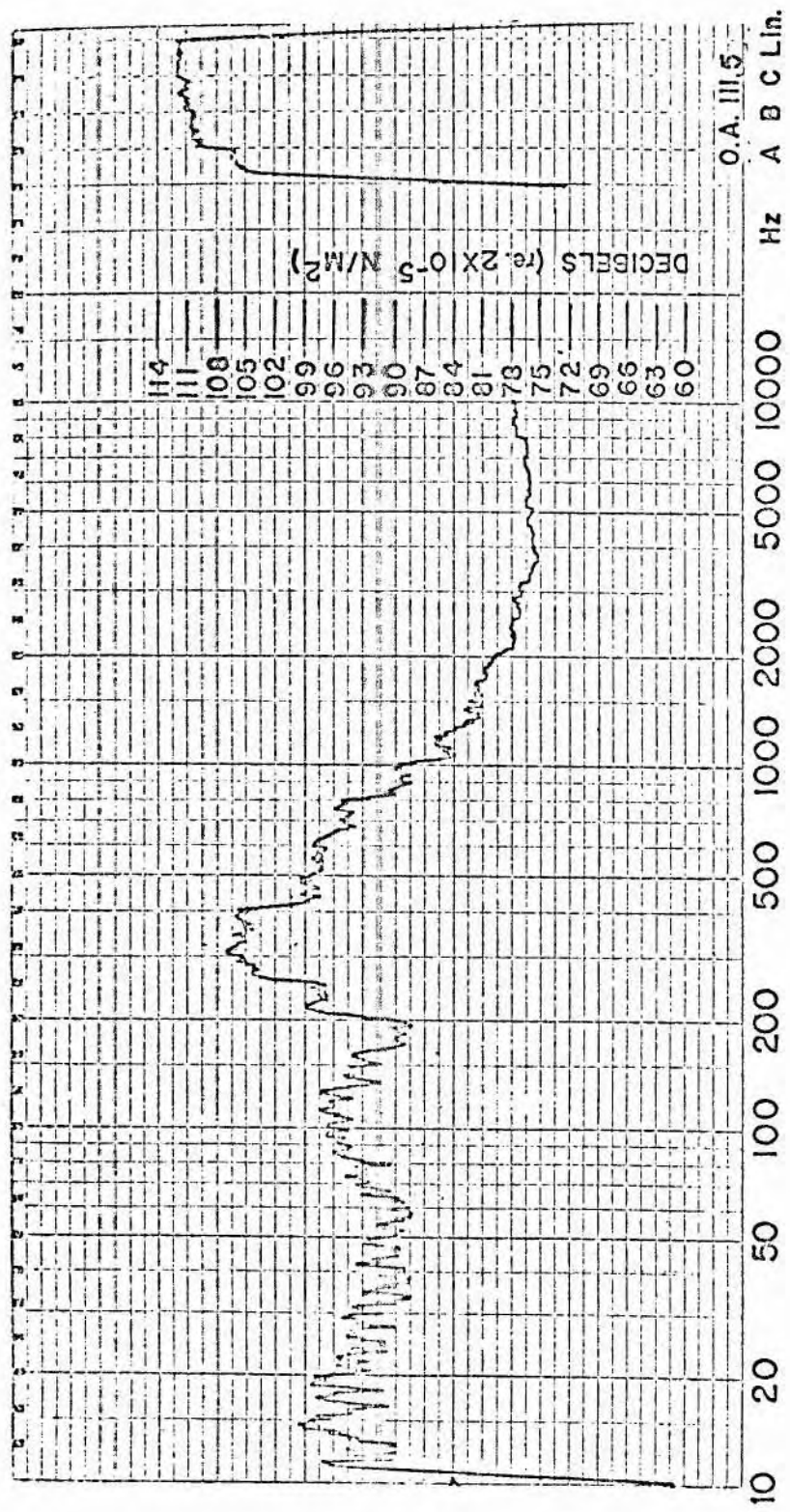
RANDOM NOISE SPECTRUM FOR TEST SPECIMEN NO. 1
IN ANECHOIC CHAMBER

FIGURE 10



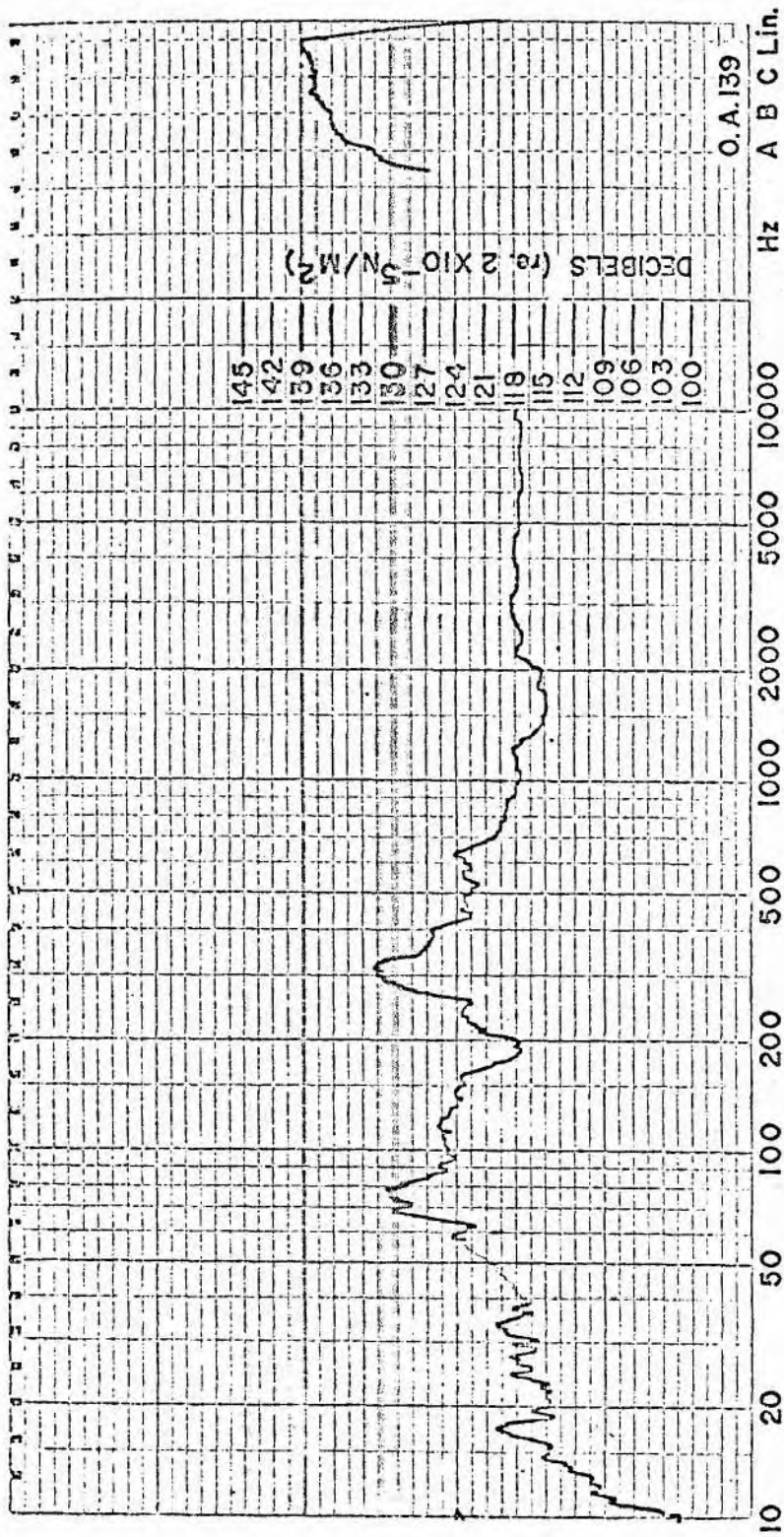
RANDOM NOISE SPECTRUM FOR TEST SPECIMEN NO. 2
IN REVERBERATION CHAMBER

FIGURE 11



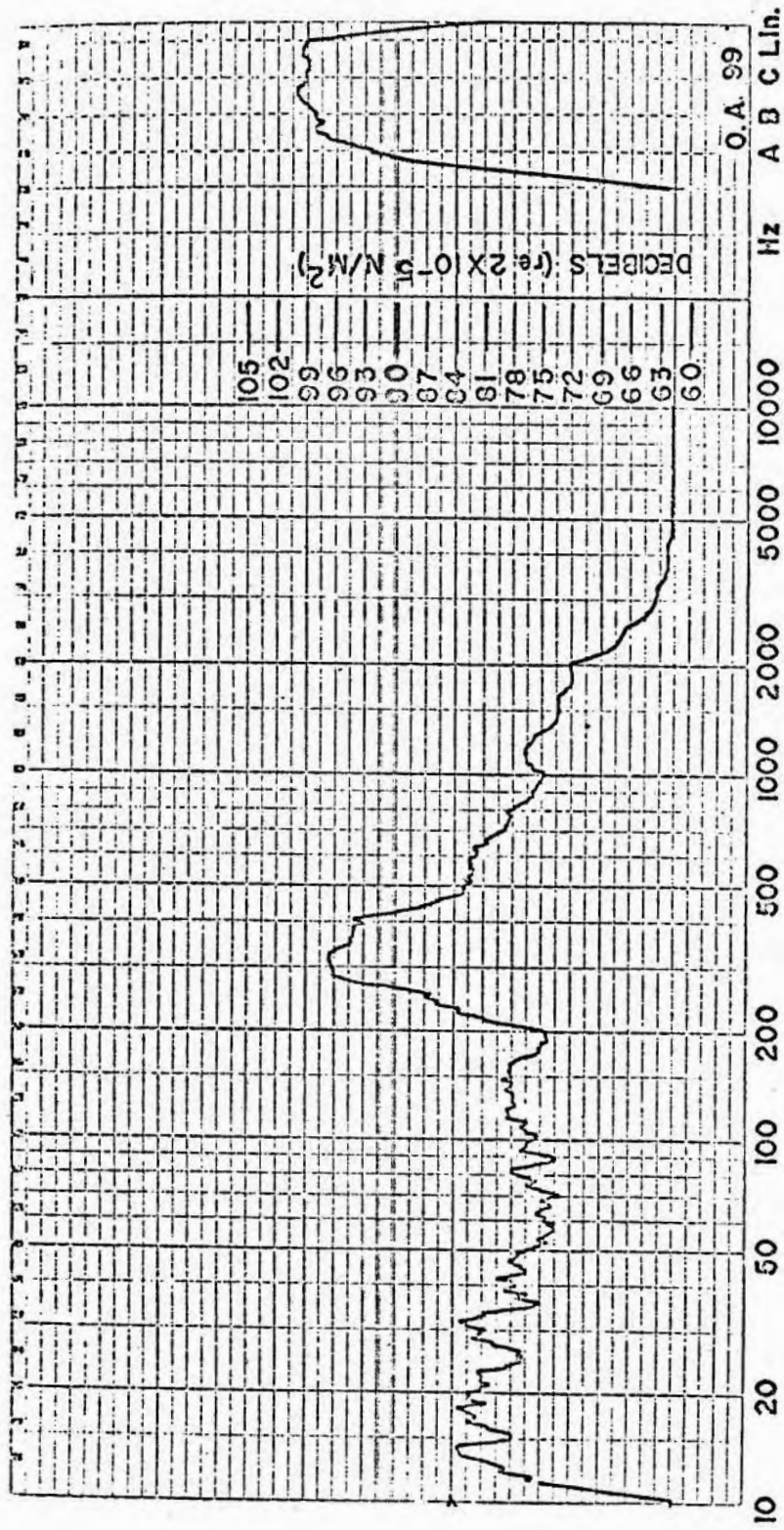
RANDOM NOISE SPECTRUM FOR TEST SPECIMEN NO. 2
IN ANECHOIC CHAMBER

FIGURE 12



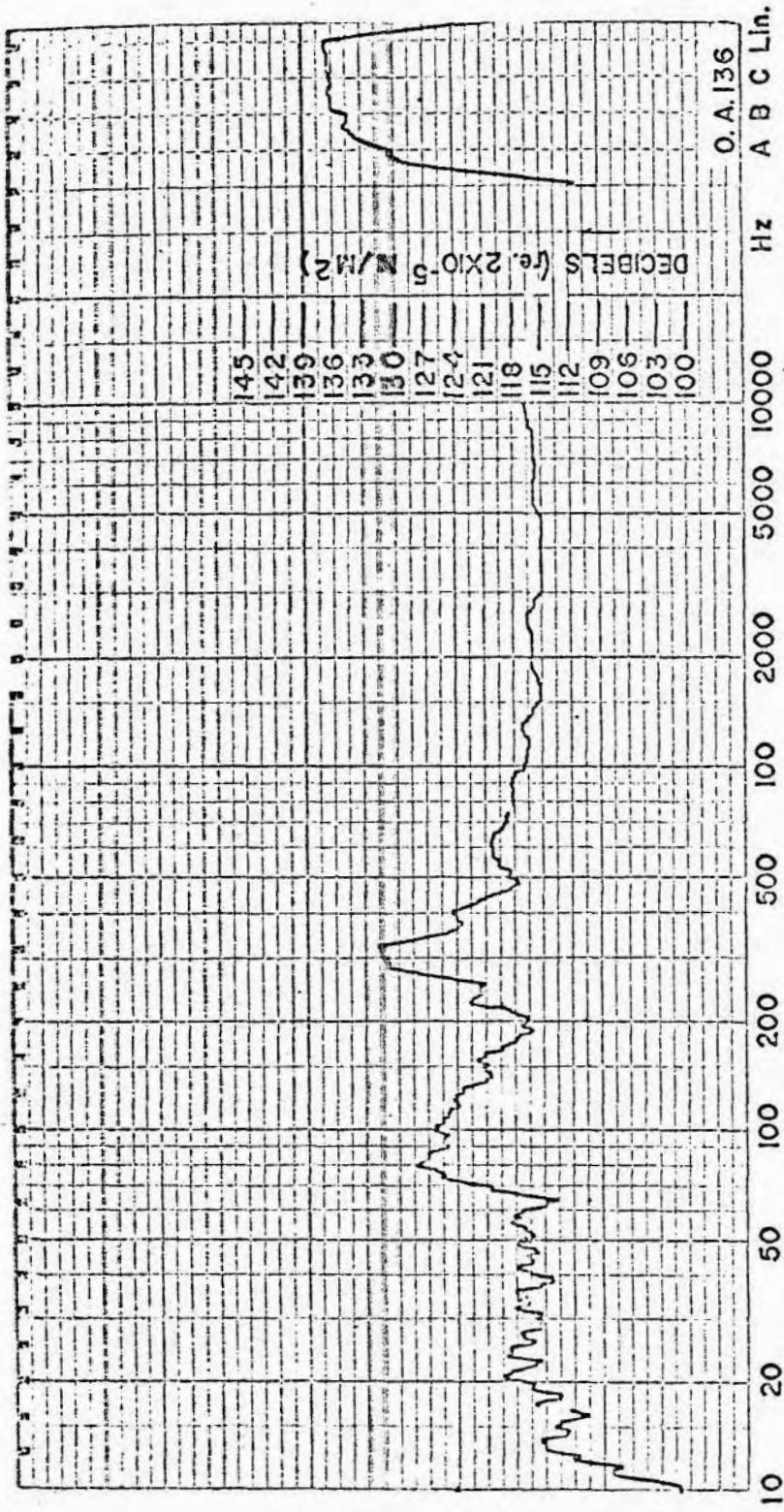
RANDOM NOISE SPECTRUM FOR TEST SPECIMEN NO. 3
IN REVERBERATION CHAMBER

FIGURE 13



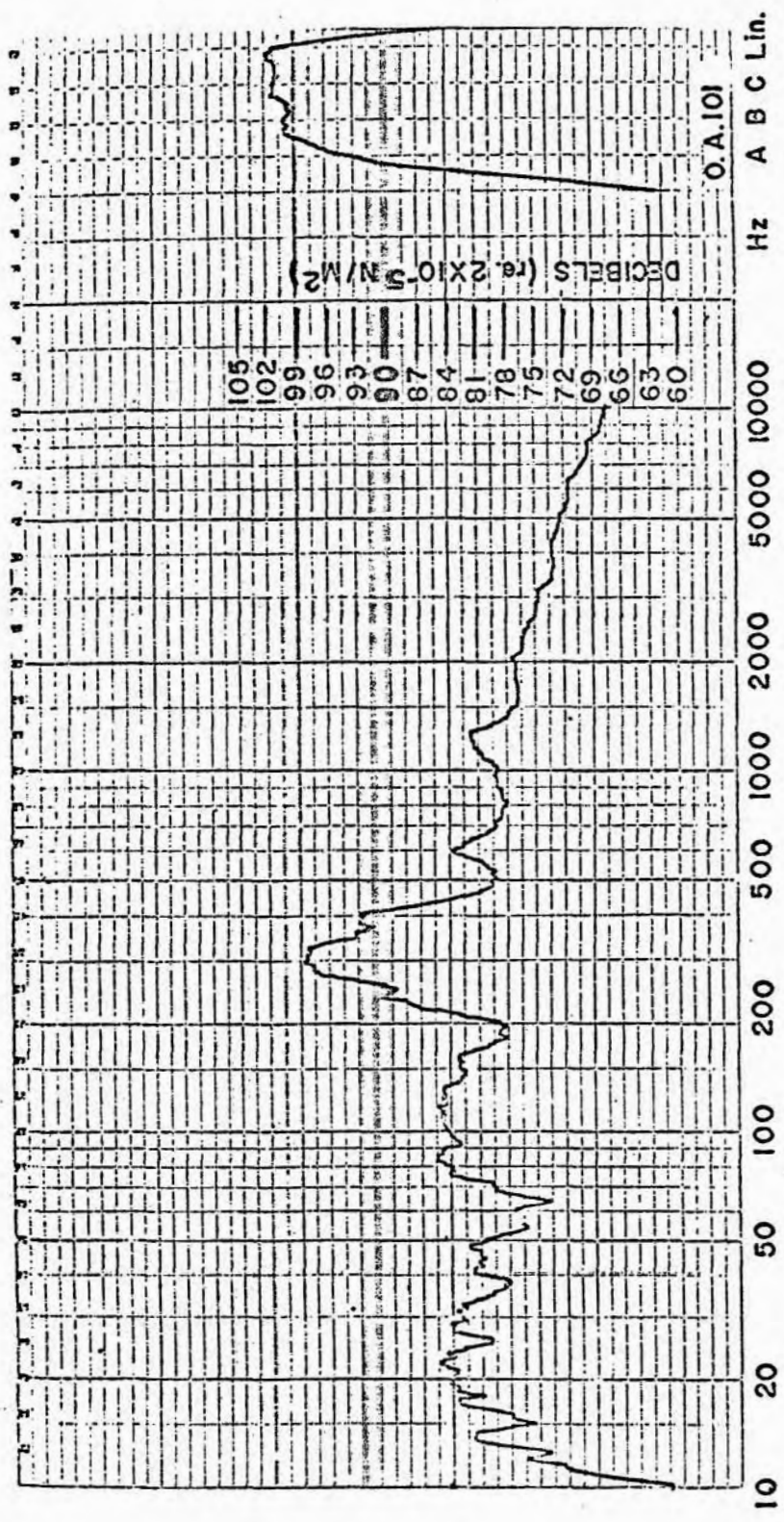
RANDOM NOISE SPECTRUM FOR TEST SPECIMEN NO. 3
IN ANECHOIC CHAMBER

FIGURE 14



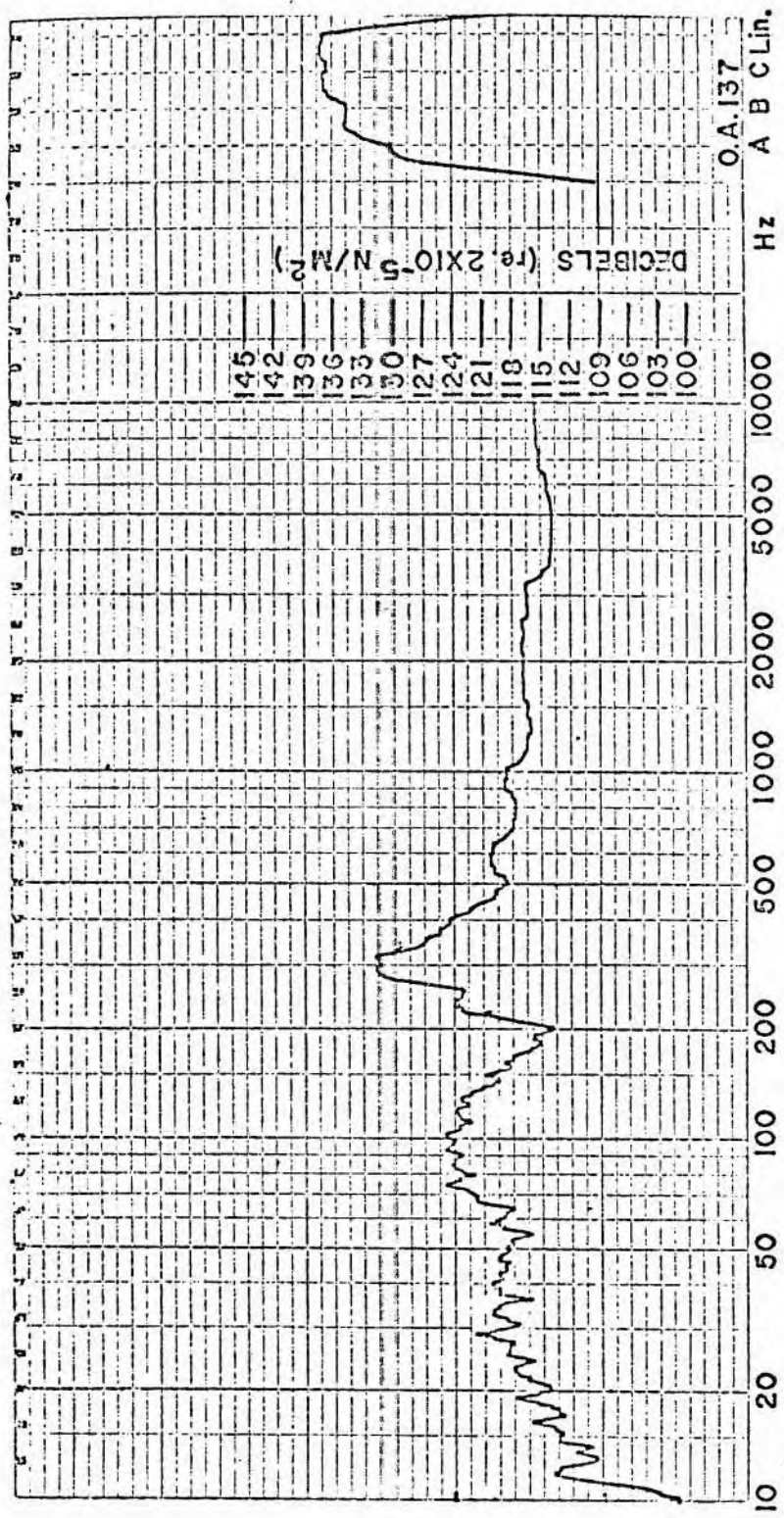
RANDOM NOISE SPECTRUM FOR TEST SPECIMEN NO. 4
IN REVERBERATION CHAMBER

FIGURE 15



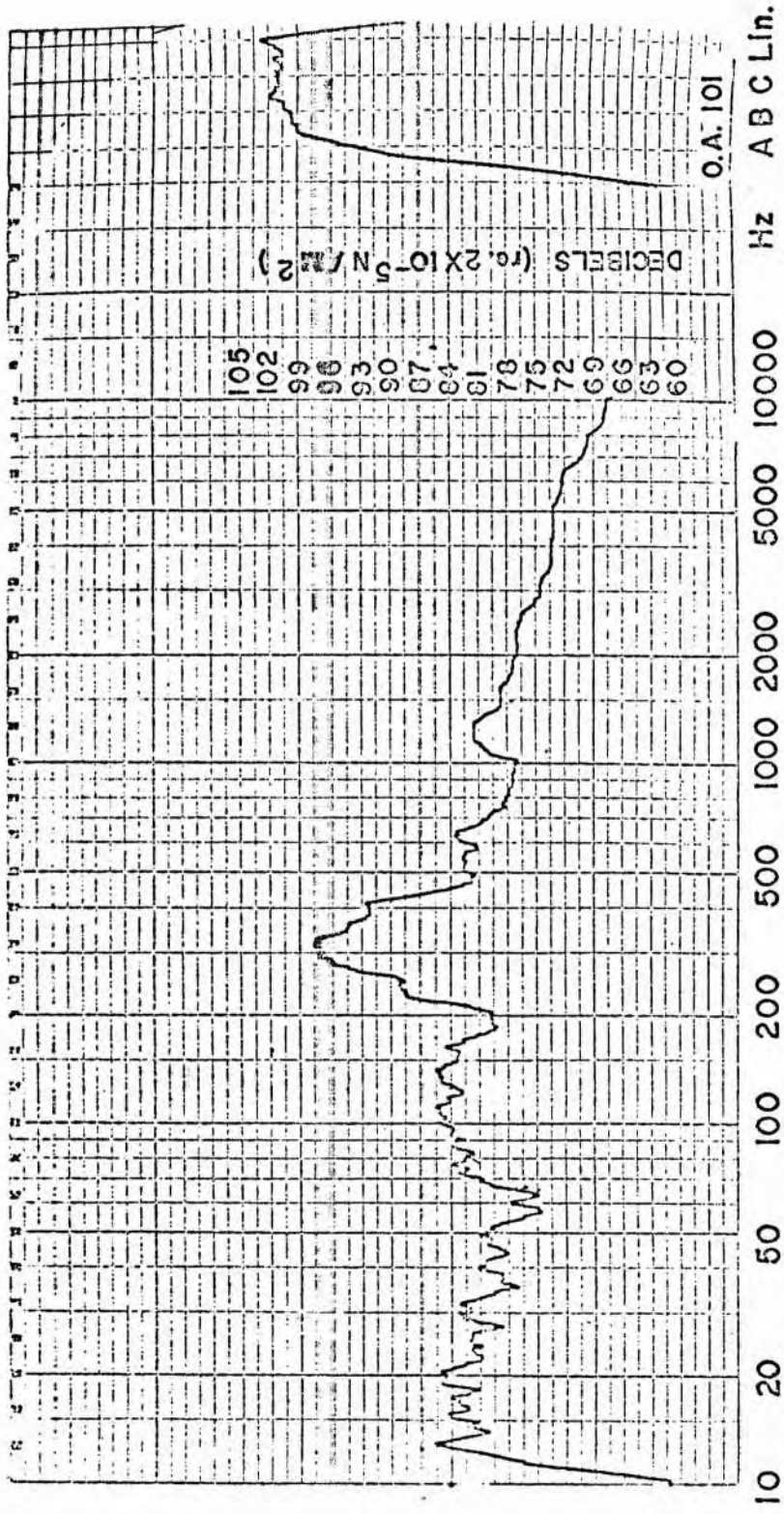
RANDOM NOISE SPECTRUM FOR TEST SPECIMEN NO. 4
 IN ANECHOIC CHAMBER

FIGURE 16



RANDOM NOISE SPECTRUM FOR TEST SPECIMEN NO. 5
 IN REVERBERATION CHAMBER

FIGURE 17

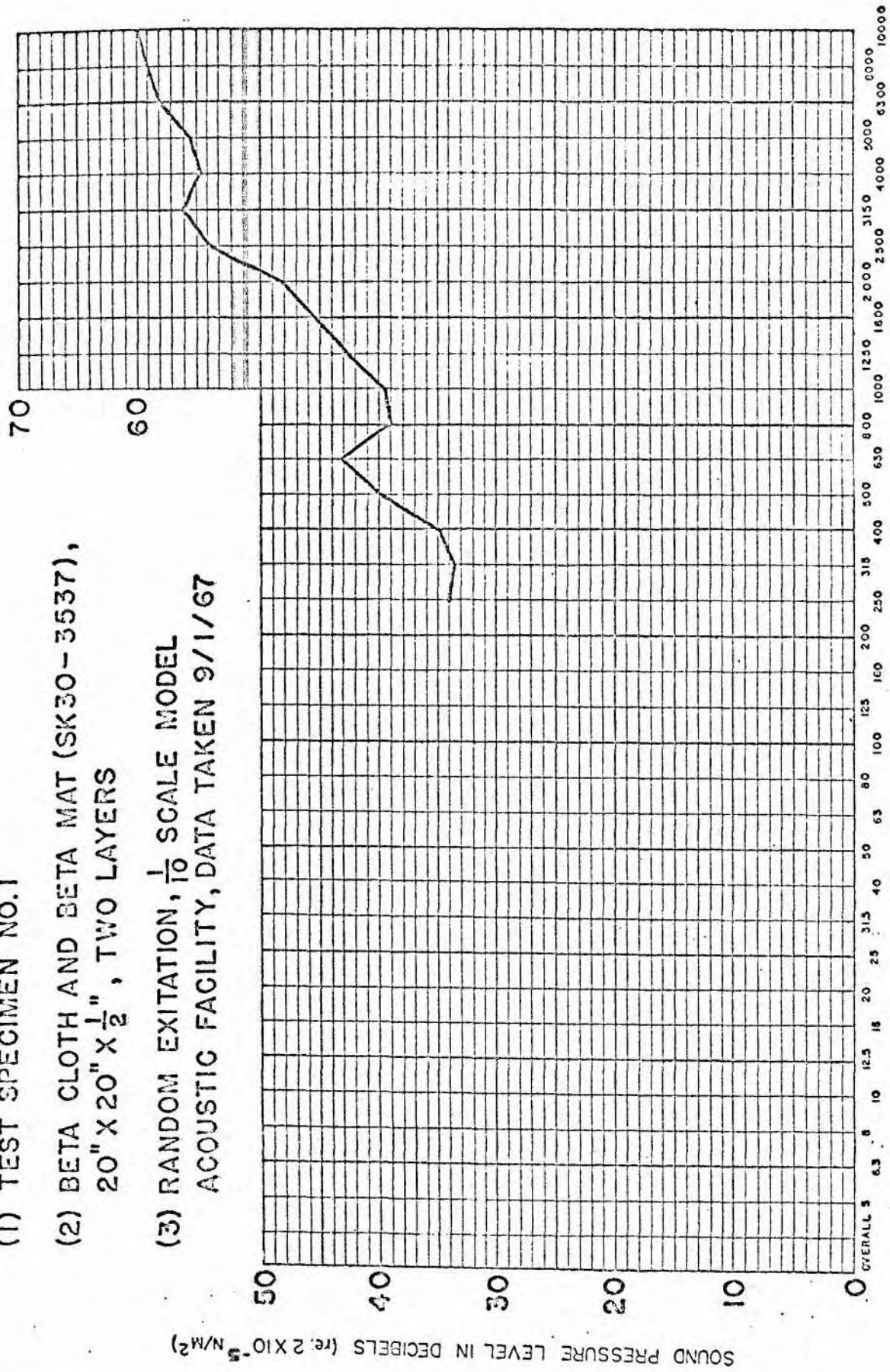


RANDOM NOISE SPECTRUM FOR TEST SPECIMEN NO. 5
IN ANECHOIC CHAMBER

FIGURE 18

NOISE REDUCTION - Random Acoustic Data

- (1) TEST SPECIMEN NO. 1
- (2) BETA CLOTH AND BETA MAT (SK30-3537),
20" X 20" X 1/2", TWO LAYERS
- (3) RANDOM EXCITATION, 1/10 SCALE MODEL
ACOUSTIC FACILITY, DATA TAKEN 9/1/67



THIRD OCTAVE BAND CENTER FREQUENCY (Hertz)

FIGURE 19

NOISE REDUCTION - Random Acoustic Data

- (1) TEST SPECIMEN NO. 2
- (2) BETA CLOTH AND ASTROQUARTZ (SK 30-3535),
20" X 20" X 1.2", THREE LAYERS
- (3) $\frac{1}{10}$ SCALE MODEL ACOUSTIC FACILITY,
DATA TAKEN 9/1/67

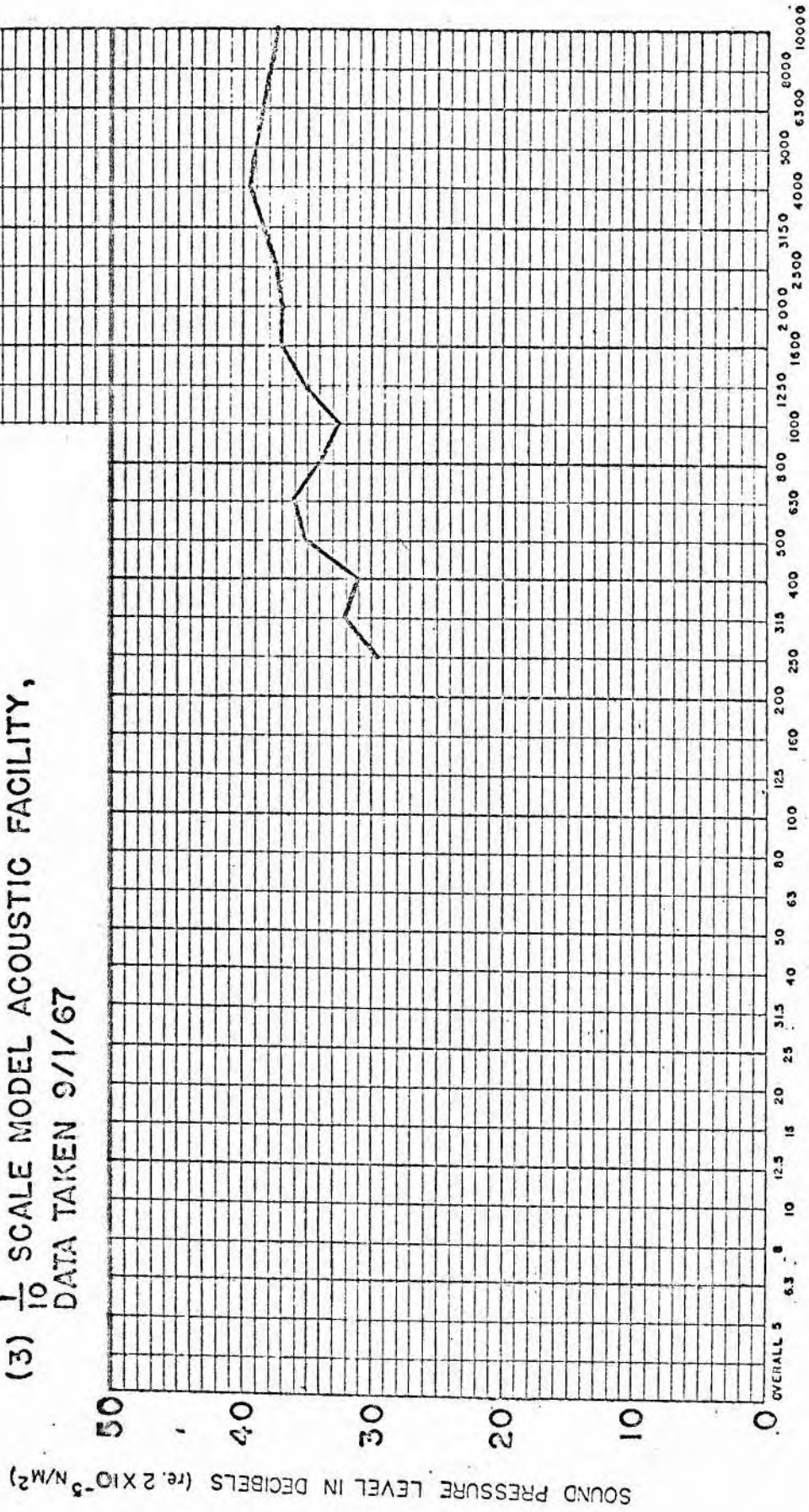


FIGURE 20

NOISE REDUCTION - Random Acoustic Data

- (1) TEST SPECIMEN NO. 3
- (2) MULTILAYER ALUMINUM FOIL AND DEXIGLASS
(NO. 0663), 19" X 19" X 1", 100 LAYERS
- (3) RANDOM EXCITATION, $\frac{1}{10}$ SCALE MODEL
ACOUSTIC FACILITY, DATA TAKEN 9/5/67

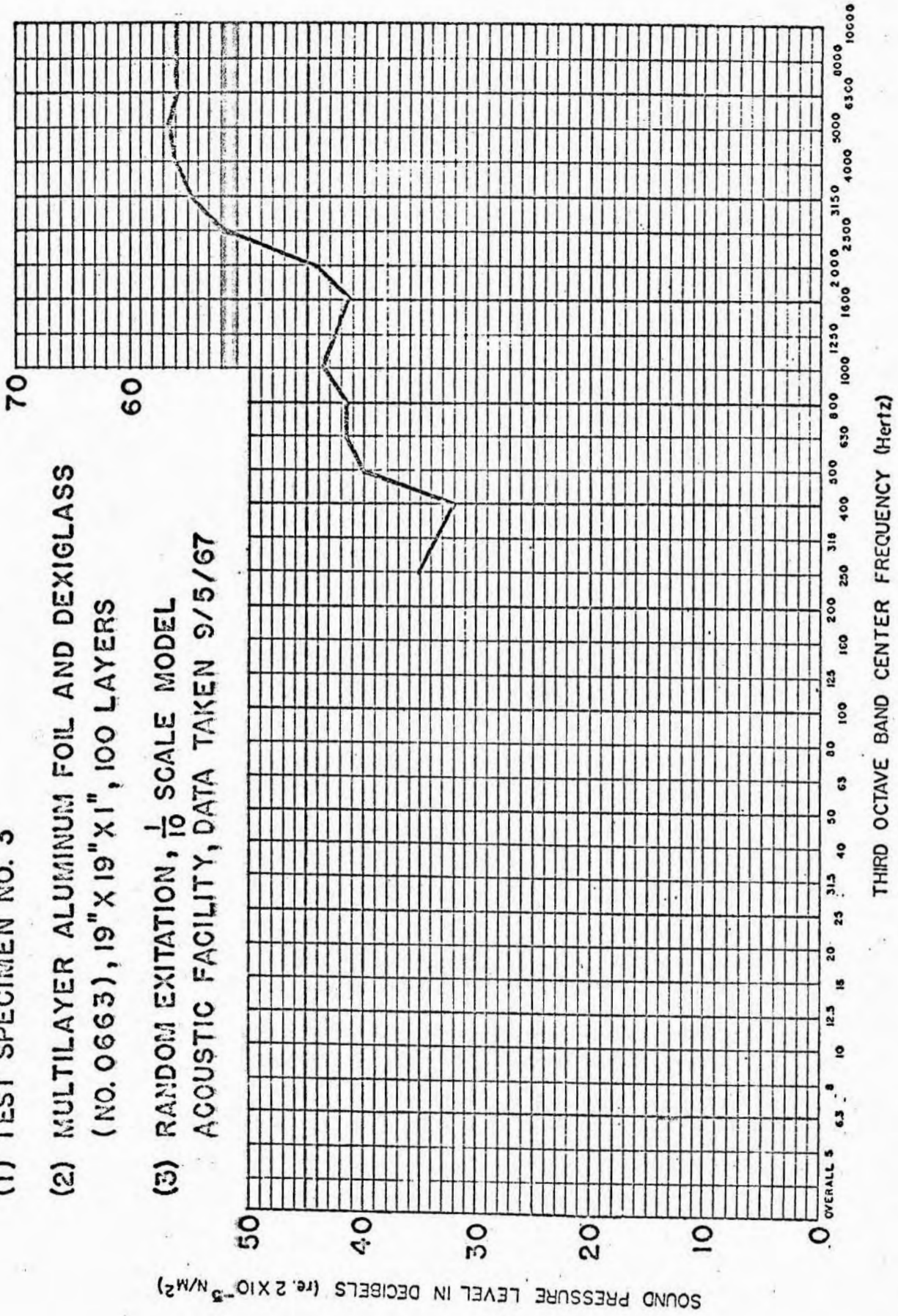


FIGURE 21

NOISE REDUCTION - Random Acoustic Data

- (1) TEST SPECIMEN NO. 4
- (2) MULTILAYER ALUMINIZED MYLAR AND URETHANE FOAM (GAC-4), 19" X 19" X 1", PLAIN, 24 LAYERS
- (3) RANDOM EXCITATION, $\frac{1}{10}$ SCALE MODEL ACOUSTIC FACILITY, DATA TAKEN 9/5/67

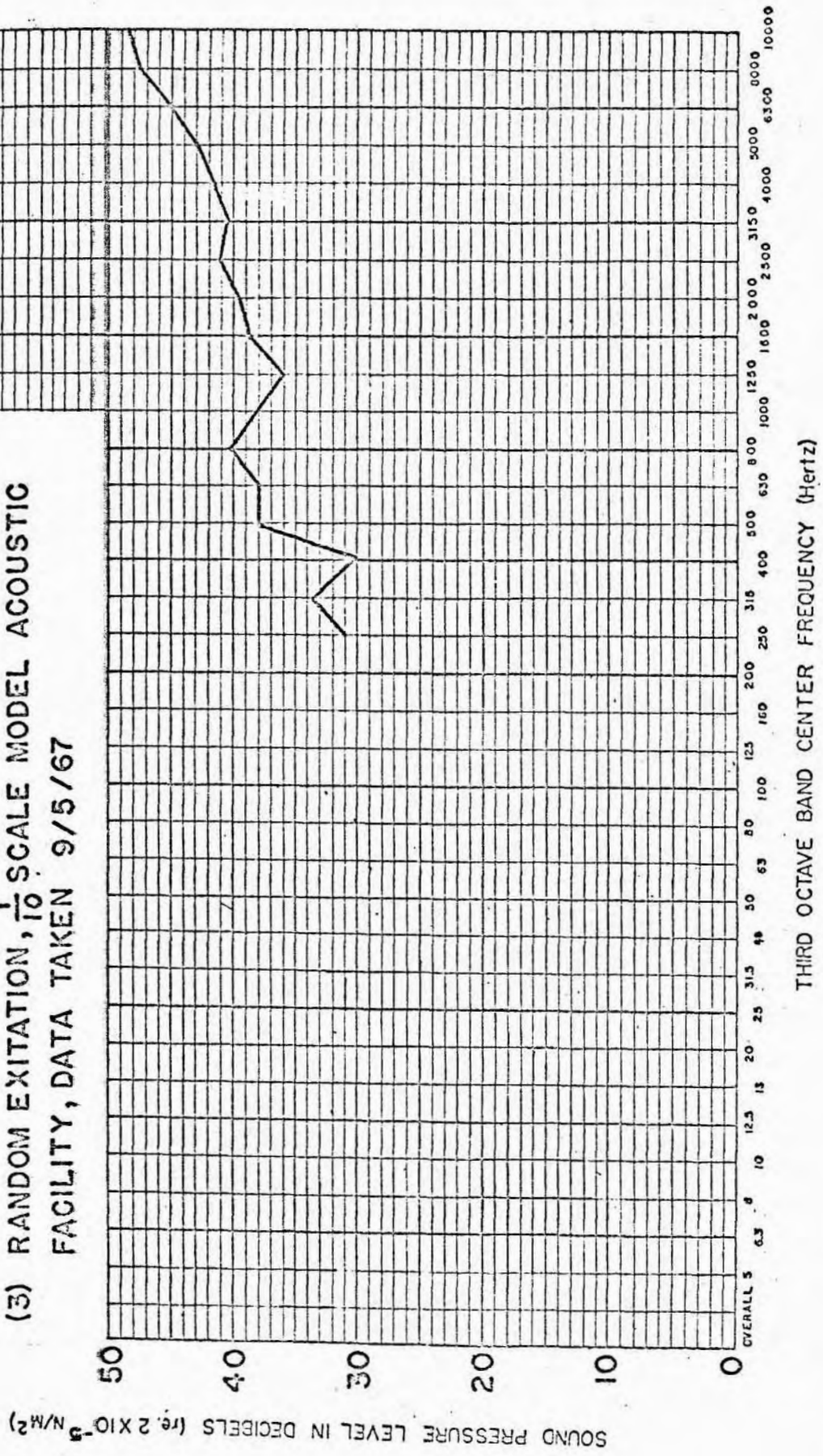
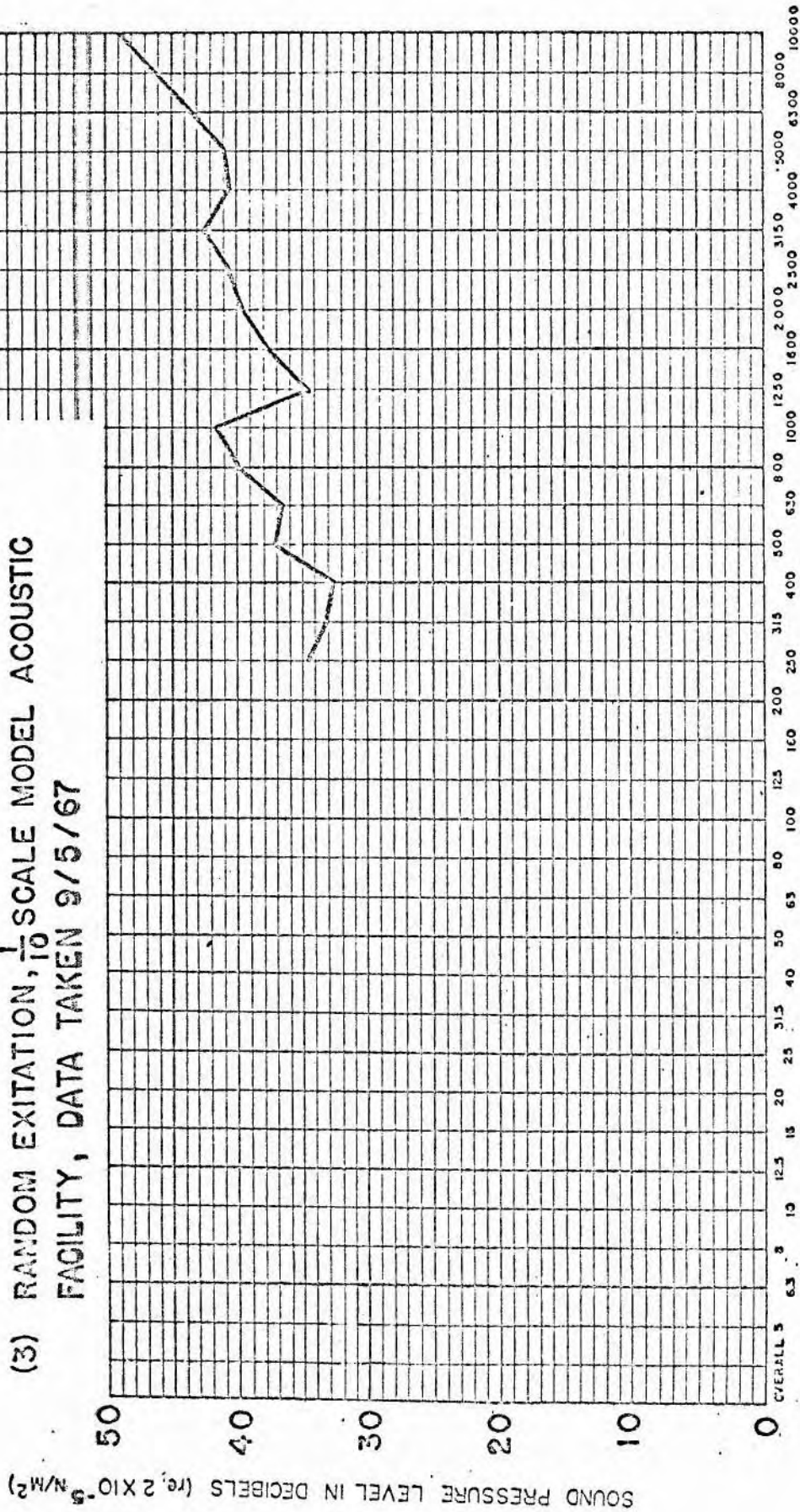


FIGURE 22

NOISE REDUCTION - Random Acoustic Data

- (1) TEST SPECIMEN NO. 5
- (2) MULTILAYER ALUMINIZED MYLAR AND URETHANE FOAM (GAC-4), 19" X 19" X 1", WITH HOLES, 24 LAYERS
- (3) RANDOM EXITATION, $\frac{1}{10}$ SCALE MODEL ACOUSTIC FACILITY, DATA TAKEN 9/5/67



THIRD OCTAVE BAND CENTER FREQUENCY (Hertz)

FIGURE 23